

Quantitative Model for the Kinetics of Compositional Intermixing in GaAs–AlGaAs Quantum-Confined Heterostructures

Amr Saher Helmy, *Student Member, IEEE*, J. Stewart Aitchison, *Member, IEEE*,
and John H. Marsh, *Senior Member, IEEE*

Abstract—A quantitative atomic-scale model for the kinetics of intermixing in GaAs–AlGaAs quantum-confined heterostructures is presented. The model takes into account the statistical nature of the defect diffusion through heterostructures and calculates its effect on the Ga–Al interdiffusion across the associated interfaces. The model has been validated by successfully predicting the observed amounts of bandgap shift induced by the process of hydrogen plasma induced defect layer intermixing, as well as for the process of impurity-free vacancy disordering using SiO₂ caps. Good agreement between calculated and measured bandgap shifts has been observed. Values of the group-III vacancy diffusion coefficient, where the agreement took place, are between 2 and $3 \times \exp[-2.72/k_B T] \text{ cm}^2 \cdot \text{s}^{-1}$.

Index Terms—Diffusion processes, quantum heterostructures, quantum-well interdiffusion, quantum wells.

I. INTRODUCTION

THE ROLE of quantum-well intermixing (QWI) in replacing regrowth and overgrowth processes for realizing optoelectronic and photonic integrated circuits (OEIC's and PIC's) has been steadily increasing ever since it was first reported in 1981 [1]. However, most work has been directed toward characterizing and optimizing the technological applications of the process. No comprehensive explanation of the mechanisms involved was presented until 1988 [2], when a quasi-equilibrium Fermi level model was developed to describe the intermixing of GaAs–AlGaAs heterostructures. Although limited modeling work has followed, it is mostly either incomplete or has only described trends rather than relating the underlying physics to experimental observations [3]–[7]. Individual factors such as the Fermi level effect, the As overpressure, as well as the other experimental parameters were correlated using basic physical relationships such as the Gibbs phase rule [8].

QWI has considerably more potential than that which has so far been exploited. It has wide spread applications in realizing mass producible OEIC's and PIC's. The resulting spatial resolution of the process control over the semiconductor bandgap has allowed extended cavity mode-locked lasers to be

realized [9]. The variation of the bandgap also allows second- and third-order nonlinear optical coefficients to be controlled, which has applications for quasi-phase-matching [10].

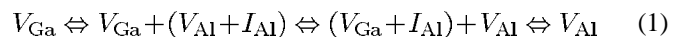
Although a number of techniques for achieving intermixing has been developed, each has certain limitations and drawbacks. Accordingly, each technique can be matched to a specific application. A comprehensive qualitative model would permit further process optimization. Such a model would not only result in improved control of existing processes such as impurity-free vacancy disordering (IFVD) in GaAs-based semiconductors, but is also necessary for extending the technology to more complicated semiconductor systems, such as IFVD in InP-based semiconductors.

Because QWI is carried out primarily at elevated temperatures through the diffusion of native point defects in the semiconductor, our model starts by studying such diffusion in the lattice. The statistical nature of the behavior of an arbitrary defect profile at elevated temperatures is modeled, and hence its contribution to the Al–Ga interdiffusion in GaAs–AlGaAs heterostructures is quantified. The approach shows promising agreement when compared with experimental results [11]. In principle, similar calculations can be performed for any intermixing technique for the GaAs–AlGaAs system.

In this paper, we start by highlighting the physical assumptions underlying the model. The process of hydrogen plasma induced defect layer intermixing (PIDLI) will then be briefly explained. The model is then used to calculate the amount of intermixing expected from the defect profile introduced by the PIDLI process, and compared with the amount of intermixing actually measured. Similar calculations and comparisons are also made for the process of IFVD. A discussion and evaluation of the developed model are then presented, followed by a summary.

II. KINETICS OF INTERMIXING

Compositional intermixing, and hence Al and Ga interdiffusion, in GaAs–AlGaAs heterostructures is either carried out directly through diffusion of group-III vacancies, V_{III} , as described by the equation,



or is assisted by the formation of group-III Frenkel defect

Manuscript received January 14, 1998; revised August 3, 1998. This work was supported by the Engineering and Physical Sciences Research Council, by Faculty of Engineering at the University of Glasgow, U.K., by an ORS award scheme in the U.K.

The authors are with the Department of Electronics and Electrical Engineering, University of Glasgow, Glasgow G12 8QQ, Scotland, U.K.

Publisher Item Identifier S 1077-260X(98)07732-6.

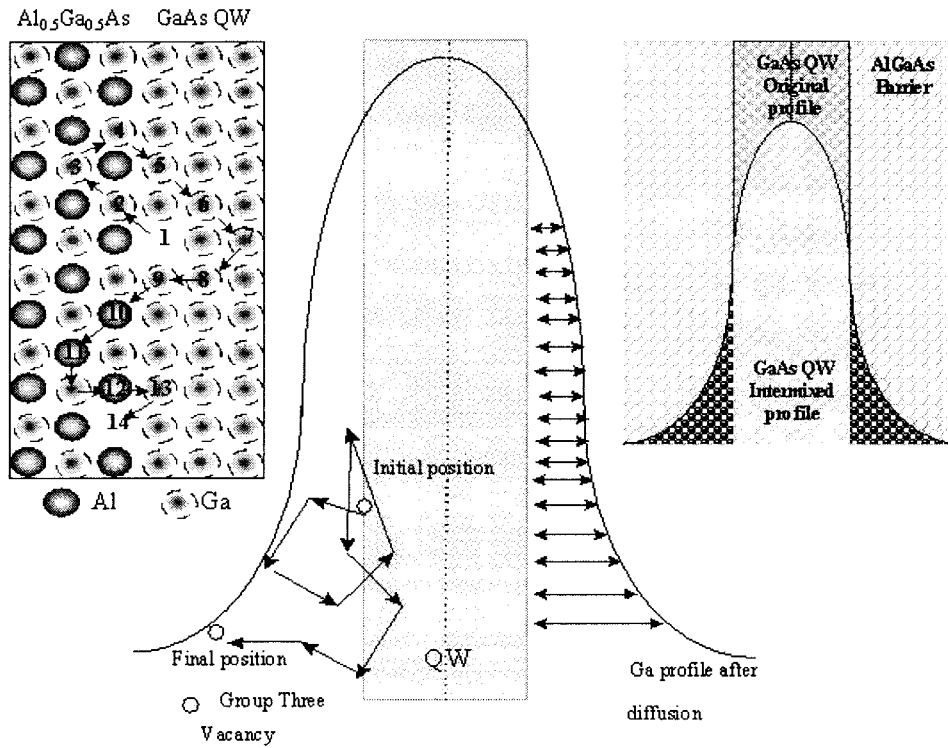


Fig. 1. Schematic diagram of the lattice hops comprised in Ga out-diffusion from the QW's, and the QW interface crossings carried out by group-III vacancies during the random walks associated with their diffusion.

pairs, through diffusion of group-III interstitials, I_{III} [2]

$$I_{Ga} \Leftrightarrow I_{Ga} + (V_{Al} + I_{Al}) \Leftrightarrow (I_{Ga} + V_{Al}) + I_{Al} \Leftrightarrow I_{Al}. \quad (2)$$

Therefore, the interdiffusion coefficient of group-III sublattice atoms through the heterostructure is dependent on the diffusion coefficient, as well as the concentration, of both group-III point defects. Each defect is created with a certain activation energy, which primarily depends on the Fermi level of the semiconductor, the As surface concentration, the ambient temperature, and the scheme by which it was created [2], [8].

Group-III point defects and Frenkel defect pairs can be introduced by various schemes. Impurity induced disordering (IID) [1], uses the dependence of the equilibrium defect concentration on the Fermi level in the semiconductor to increase the number of group-III defects. IID, however, introduces excessive free carrier absorption [12]. Implantation defect induced disordering [13], PIDLI [14], and pulsed photoabsorption induced disordering, P-PAID [15], utilize point defects and Frenkel defect pairs introduced by the interaction between the lattice atoms in the semiconductor and the implanted ions, plasma ions, and photons respectively, to enhance Ga–Al interdiffusion. Limitations then arise due to other types of defects introduced by these processes. Line defects and dislocation loops are examples of defect types which are not annealed out at elevated temperatures, and can act as sinks for point defects [16]. On the other hand, IFVD uses the group-III vacancies introduced due to Ga out-diffusion into dielectric caps at elevated temperatures to assist Ga–Al interdiffusion [17]. IFVD has been utilized extensively to fabricate OEIC's and PIC's, due to its simplicity and the resulting low optical losses [12], [18]. A given defect profile will diffuse through

the lattice while being thermally processed. In the rest of this section a method of calculating the diffusion coefficient associated with a given vacancy profile at the QW will be developed. The resulting diffusion coefficients can then be directly related to the shift in the photoluminescence (PL) wavelength resulting from a bandgap shift, as will be explained later.

Since we are interested in the kinetics of the interactions between point defects and lattice atoms, investigating the statistical behavior of the point defect diffusion will reveal the underlying physical mechanisms more comprehensively. The diffusion of a defect within the lattice can be considered as a number of hops carried out in a random walk. In Fig. 1, the random walk is illustrated along with the resultant diffusion length. The diffusion coefficient can be expressed as [19]

$$D_{vac} = \frac{f \cdot w_v}{2} \left(\frac{a_o}{2} \right)^2 \quad (3)$$

where w_v is the effective defect hop frequency, a_o is the lattice constant of GaAs, and $a_o/2$ is the hop length, given that the group-III point defects will primarily diffuse on the group-III sublattice. The factor f is the reciprocal of the number of directions of the nearest neighboring sites to which the vacancy can hop. For three-dimensional diffusion in the crystal, f is equal to 1/3. This picture suggests that within the regions where $[V_{III}] \gg [I_{III}]$ diffusion is determined primarily by vacancies. It should be also noted that the background equilibrium concentration of V_{III} ought to be taken into consideration if it was found to have a significant effect on the amount of intermixing induced. However, the reported V_{III} background equilibrium concentration in undoped QW's

is equal to $1.25 \times 10^{31} \exp[-3.28/k_B T] \text{ cm}^{-3}$, which has no significant effect on the amount of intermixing induced at annealing temperatures below 1000 °C.

- 1) Prior to annealing, GaAs–AlGaAs heterostructures have an abrupt change in the Ga concentration at the interface. In the presence of a given concentration of group-III defects, at elevated temperatures Ga–Al interdiffusion will take place across the interface, giving rise to an error function-like profile. Assuming a GaAs–AlAs heterostructure, the Ga profile can thus be expressed as

$$C_{\text{QW}} = \frac{C_o}{2} \operatorname{erfc} \left[\frac{z - L_z/2}{2\sqrt{D_{\text{QW}}t}} \right] \quad (4)$$

where C_{QW} and D_{QW} are the concentration and the diffusion coefficient of Ga atoms out-diffused from the QW, respectively, C_o is their initial concentration in the wells, L_z is the QW thickness, and z is the spatial depth parameter. The movement of Ga atoms takes place through vacancy diffusion, therefore, the profile of the diffused Ga arises from a certain number of discrete lattice hops. The number of lattice hops can be obtained by integrating the spatial parameter over all the Ga concentration outside of the well boundary, and normalizing it with respect to the lattice hop length, as shown in Fig. 1. The number of lattice hops required to achieve a given diffusion profile is calculated from

$$N_{\text{QW}} = \frac{k}{a_o/2} \int_0^{C_{\text{QW}}(L_z/2)} z(C_{\text{QW}}) d(C_{\text{QW}}) \quad (5)$$

$$z(C_{\text{QW}}) = 2\sqrt{D_{\text{QW}}t} \operatorname{erfc}^{-1} \left[\frac{2C_{\text{QW}}}{C_o} \right] \quad (6)$$

where $C_{\text{QW}}(L_z/2)$ is the concentration of Ga at the edge of the well. This means that if we are able to predict a number of lattice hops generated by diffusion of a given V_{III} profile, then by substituting this value as N_{QW} and solving (5), one can obtain an associated value for D_{QW} . Because we study a single heterostructure interface to calculate the number of lattice hops, the diffusion profile is an erfc, whereas for a QW (or a double QW) the diffusion profile is a superposition of the erfc profiles at every interface [20], [21].

The expression for N_{QW} above was found, however, for a GaAs–AlAs interface, under the assumption that the Ga concentration in the barriers always remains sufficiently small that every Ga atom out-diffusing from the well is replaced by an Al atom from the barrier. When the barrier Al concentration is not $\sim 100\%$, the fluxes of Ga and Al will change by a factor depending on their concentrations in the atomic layers on either side of the QW/barrier interface. Therefore, a factor k is introduced in (6) to account for the fact that the Al concentration in the barrier will not generally be 100%; (k is equal to unity in case of a GaAs–AlAs heterostructure). k also accounts for the changes in Ga and Al concentrations at the interface as intermixing takes place. The factor k is equal to $1/(x_{\text{Al}}^{\text{barrier}}(t) \cdot x_{\text{Ga}}^{\text{well}}(t))$, where $x_{\text{Ga}}^{\text{well}}(t)$ and $x_{\text{Al}}^{\text{barrier}}(t)$ are the time

dependent Ga and Al concentrations in the atomic layers on either side of the QW/barrier interface normalized by C_o , the concentration of group-III atoms in the lattice. When added to N_{QW} the expression then represents the actual number of lattice hops, by taking into account the finite probability of an Al atom diffusing from the barrier to the QW, and of it being replaced by a Ga atom out-diffusing from the QW to the barrier.

After calculating the number of lattice hops induced by a given vacancy concentration, we substitute for N_{Ga} in (5) and solve to give the corresponding D_{QW} . The PL shifts resulting from this calculated diffusion coefficient can then be obtained and compared with the experimental ones. PL shifts corresponding to a given diffusion length are calculated by solving the Ga diffusion equation in a QW in conjunction with the Schrödinger wave equation to obtain the confined energy levels for a given diffusion length [20]. The Ga diffusion is assumed to follow Fick's law resulting in a diffusion profile represented by double erfc.

To calculate the number of lattice hops induced by a given vacancy concentration, we therefore need to study the effect of V_{III} on a heterostructure interface during annealing.

- 2) At the interface of a heterostructure, each time a V_{III} crosses the plane into the QW's, a Ga atom moves one lattice site, in the opposite direction, out of the well into the barrier. A subsequent uncorrelated interface crossing of a V_{III} in the opposite direction is needed to transport an Al atom one lattice site toward the well, as illustrated in (1). Therefore on average, for each two crossings of the barrier/QW interface carried out by V_{III} , one Al atom can move one lattice hop toward the interface eventually replacing the out-diffused Ga atom. In the calculations reported here, we assume $[V_{\text{III}}]$ is the same at both interfaces of a particular QW.

The total number of barrier/QW interface crossings undertaken by the atoms, N_{IC} , will therefore correspond to the total number of lattice site-hops available for the Al–Ga interdiffusion, which can be calculated for a time span t by

$$N_{\text{IC}} = \int_0^t \frac{w_v}{2} \cdot N_v(d_{\text{QW}}, t) \cdot dt \quad (7)$$

where $N_v(d_{\text{QW}}, t)$ is the time dependent V_{III} concentration at one of the QW interfaces. For a given vacancy concentration $N_v(d_{\text{QW}}, t)$ generated by any means, the model predicts N_{IC} lattice hops are available for group-III interdiffusion across that interface. The value of N_{IC} calculated from the model above is therefore the same as N_{QW} in (6), and hence the corresponding values of D_{QW} and $L_{D_{\text{QW}}}^2$ for a given vacancy profile, $N_v(d_{\text{QW}}, t)$, can be calculated, from which the PL shift predicted is obtained [20].

Within the rest of the paper the validity of the model is demonstrated through the agreement between the calculated and measured PL shifts calculated from the diffusion coefficient as discussed above.

III. KINETICS OF PIDLI

PIDLI is based on multiple cycles of exposing heterostructure samples to hydrogen plasma in an RIE machine, followed by thermal processing in a rapid thermal annealer (RTA). Bandgap shifts in excess of 40 meV have been achieved with such a process in eight cycles [14]. RIE damage has adverse effects on many devices, and in particular metal–semiconductor field-effect transistor (MESFET's) where it was discovered that it caused a reduction of the transconductance when gate recess etching had been carried out using RIE [22]. Irradiation damage is caused by the hydrogen ions in the plasma impinging on the semiconductor surface during the plasma exposure. Energy is, therefore, transferred to the lattice, introducing point defects [23], mainly interstitials resulting from the incident ions and neutrons, or lattice atoms knocked off due to the momentum transfer. There can also be vacancies resulting from the knocked off atoms, the vacancies being created where the knock off has occurred.

The defect profile produced by a RIE process similar to PIDLI, based on a H_2/CH_4 plasma, has previously been studied and characterized [24]. Phenomenological expressions for the defect profile have been obtained. The distribution function of the defects can be written as

$$N(z, v(t - t_o)) = \frac{\lambda g_o}{v} \exp[-(z - v(t - t_o))/\lambda] \cdot (1 - \exp[-v(t - t_o)/\lambda]) \quad (8)$$

where z is the distance from the surface of the semiconductor, v is the etch rate in $nm \cdot s^{-1}$, t is the plasma exposure time, g_o with dimensions of $cm^{-3} \cdot s^{-1}$ is a parameter related to the number of bombarding ions, and λ with dimensions of nm is dependent on the ion energy. In the referenced work, the defects studied were deep level traps, quantified through quantum wire conduction measurements. The concentration of group-III defects is expected to have the same functional dependence as that of the deep level defects, since both are created by hydrogen ion bombardment [11]. Therefore, (9) was assumed to give the initial vacancy profile in our calculations. By integrating (9) and substituting the numerical values of the parameters quoted for the H_2/CH_4 RIE process with the exposure time of the PIDLI process, which is 40 s, the sheet density of induced defects is [25]

$$C_{\text{defects}}(z) = 5.6 \times 10^{12} \exp[-z/3 \times 10^{-6}] \text{ cm}^{-2}. \quad (9)$$

Vacancies and interstitials will be created in almost equal numbers during plasma exposure. Although a fraction of these will recombine instantaneously, the diffusion coefficient of interstitials is sufficiently large, even at room temperature [4], to allow some of them to diffuse into the bulk of the sample, leaving behind a vacancy profile given by (9). It should be noted that diffusion of interstitials alone does not necessarily lead to significant intermixing, as can be seen from (2). At elevated temperatures, the vacancies' behavior will be primarily governed by their diffusion into the bulk of the semiconductor and by their annihilation at the semiconductor surface. Because of the large concentration gradient immedi-

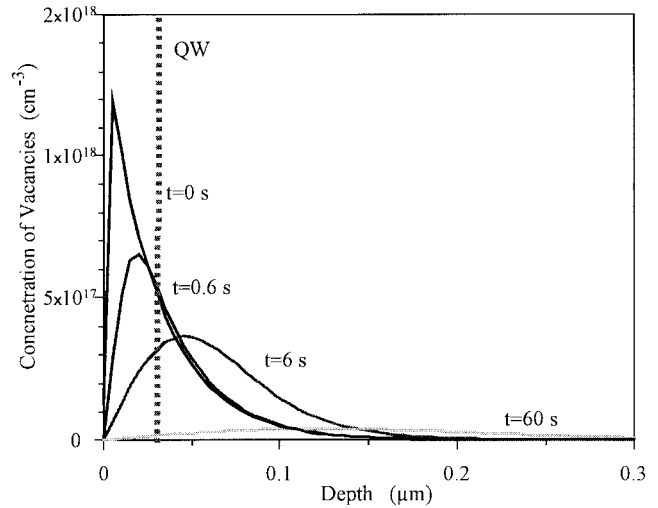


Fig. 2. Plot for the group-III vacancy concentration in the GaAs–AlGaAs single QW structure for different annealing time spans for the PIDLI process. The surface recombination velocity of group three vacancies used in the calculations is $0.1 \mu\text{m} \cdot \text{s}^{-1}$.

ately below the surface, the preferential direction of diffusion, dictated by the derivative of the concentration gradient, will be toward the surface rather than toward the substrate. The concept of recombination of carriers at the surface with a certain recombination velocity has been adopted, in the model, to describe the annihilation of vacancies at the surface of the semiconductor exposed to the hydrogen plasma in the PIDLI. At the surface, vacancies will hence have a surface release velocity v_{PIDLI} . The diffusion equation governing the behavior of the vacancies and the appropriate boundary conditions, can be expressed as

$$\frac{\partial}{\partial z} D_{\text{vac}} \frac{\partial C_{\text{vac}}}{\partial z} = \frac{\partial C_{\text{vac}}}{\partial t} \quad (10)$$

$$\text{@}t = \infty \rightarrow C_{\text{vac}} = 0$$

$$\text{@}t = 0 \rightarrow C_{\text{vac}} = C_{\text{defects}}(z)$$

$$\text{@}z = l \rightarrow V_{\text{PIDLI}} C_{\text{vac}} = D_{\text{vac}} \frac{\partial C_{\text{vac}}}{\partial z}. \quad (11)$$

Solutions for such a boundary value problem are obtained according to Sturm–Liouville theory [26]. In this approach, the time varying concentration profiles are expanded as a series of orthogonal trigonometric functions, such that

$$Nv(z, t) = \sum_{n=1}^{\infty} k_n \cdot \sin[\lambda_n z] \exp[-\lambda_n^2 D_{\text{vac}} t] \quad (12)$$

$$k_n = \frac{\langle C_{\text{defects}}(z) \cdot \sin[\lambda_n z] \rangle}{\langle \sin[\lambda_n z] \cdot \sin[\lambda_n z] \rangle} \quad (13)$$

$$\lambda_n \Rightarrow n\text{th root of: } \tan[l \cdot \lambda_n] = \frac{-\lambda_n \cdot D_{\text{vac}}}{v}. \quad (14)$$

The diffusion profile of $Nv(z, t)$ is shown in Fig. 2. The predicted number of lattice hops contributing to intermixing, N_{IC} , can then be calculated from (5) using the reported process parameters [24].

To obtain N_{Ga} , the number of lattice hops calculated from the experimentally observed PL shifts, an experiment has been

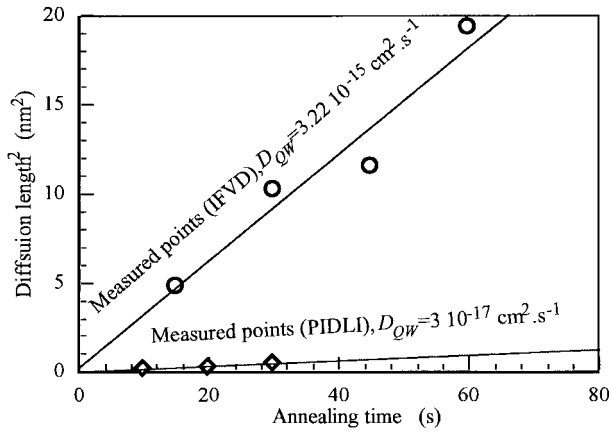


Fig. 3. Plot for the square of the diffusion length and the anneal time for the both the PIDLI and IFVD processes. The slope of the line passing through the measured points is approximately constant giving a value of D_{QW} equal to $3 \times 10^{-17} \text{ cm}^2 \cdot \text{s}^{-1}$ for the PIDLI process, and equal to $3.22 \times 10^{-15} \text{ cm}^2 \cdot \text{s}^{-1}$ for the IFVD process.

carried out to measure the diffusion coefficient of Ga out-diffusing into the barriers. This diffusion coefficient can then be used to calculate from (6). The wafer used was grown on a n-type GaAs substrate with a shallow QW placed at a depth of 30 nm. Starting from the substrate, an undoped GaAs buffer layer of 100 nm was grown followed by 500 nm of n-type $\text{Ga}_{0.63}\text{Al}_{0.37}\text{As}$ doped to $7 \times 10^{16} \text{ cm}^{-3}$. The QW, 5 nm of undoped GaAs, was then grown followed by 2 nm of AlAs, and 20 nm of p-type $\text{Ga}_{0.63}\text{Al}_{0.37}\text{As}$ doped to $7 \times 10^{16} \text{ cm}^{-3}$, and a 10-nm GaAs p^+ cap. Samples of area $3 \text{ mm} \times 3 \text{ mm}$ were then exposed to a single cycle of the plasma and annealed for different time spans, namely 10, 20, and 30 s at $875 \text{ }^\circ\text{C}$. The PL spectra of the samples were then measured, from which the diffusion length was obtained by solving Al/Ga diffusion equations in conjunction with the Schrödinger wave equation for the QW [20]. Upon plotting the square of the diffusion lengths against time, as shown in Fig. 3, the relation was found to be linear. This produces a time invariant Ga diffusion coefficient for the PIDLI process, within the range of anneal times used and for that QW depth. The slope of the line is directly proportional to the diffusion coefficient, $L_{D_{QW}}^2 = D_{QW}t$, hence the Ga diffusion coefficient was found to be $3 \times 10^{-17} \text{ cm}^2 \cdot \text{s}^{-1}$. Using the reported value for D_{vac} [3], which is $1.13 \times 10^{11} \text{ cm}^2 \cdot \text{s}^{-1}$ at $875 \text{ }^\circ\text{C}$, the value of w_v can be obtained from (3), and was found to be $2.8 \times 10^3 \text{ hop} \cdot \text{s}^{-1}$. Because $N_v(d_{QW}, t)$ is now known, N_{IC} and the associated PL shifts calculated from the model can be compared to those measured.

During diffusion, vacancies will be annihilated at the free surface of the semiconductor, i.e., the probability of a vacancy being reflected is almost negligible. The expected vacancy surface release velocity v is, therefore, effectively infinity. The saturation effect of the surface recombination velocity on N_{IC} is seen in the model for values of v larger than $1 \times 10^{-4} \text{ cm} \cdot \text{s}^{-1}$ [11]. It was found that the PL shifts predicted by the model for the PIDLI process have an order of magnitude agreement with experiment carried out at $875 \text{ }^\circ\text{C}$, for surface

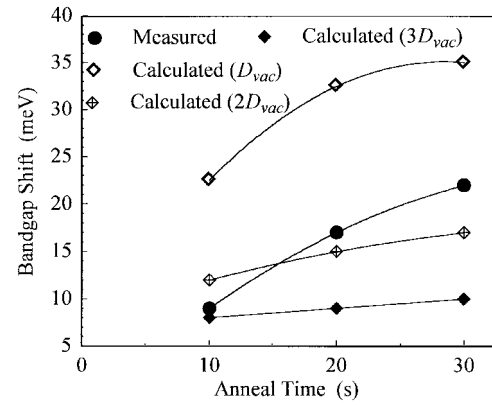


Fig. 4. Plot for measured and calculated PL shifts resulting from the PIDLI process in a shallow single QW for different values of D_{vac} .

recombination velocities larger than $1 \times 10^{-4} \text{ cm} \cdot \text{s}^{-1}$ as can be seen in Fig. 4. In other words, the PL shifts predicted by the model agree best when v tends to infinity, which was expected for the condition of the semiconductor surface after the plasma exposure in the PIDLI process. However, if the value of D_{vac} is increased, better agreement between the calculated and measured values is achieved, as can also be seen in Fig. 4. When D_{vac} increases, the resulting intermixing decreases because $[V_{III}]$ take place in the vicinity of the QW for shorter time spans due to its more rapid diffusion out of the sample. For v equal $1 \times 10^{-4} \text{ cm} \cdot \text{s}^{-1}$ and a value for D_{vac} , twice the reported value, $1.13 \times 10^{11} \text{ cm}^2 \cdot \text{s}^{-1}$ at $875 \text{ }^\circ\text{C}$, the measured PL shifts are in close agreement with that predicted from the model. The variation of the reported values of D_{vac} can be ascribed to the indirect means by which these measurements are done [33]. This gives room for much uncertainty in the reported values. Therefore, suggesting a factor of 2 change in D_{vac} is within reasonable error of the reported value.

IV. KINETICS OF IFVD

IFVD utilizes Ga out-diffusion into dielectric caps at elevated temperatures to introduce group-III point defects [27]. Since its discovery [28], it has been widely used to fabricate OEIC's and PIC's [12], [14]. It can be readily understood from the mechanism that the defect type introduced is the Schottky defect, specifically V_{III} . The concentration of Ga atoms out-diffused in dielectric caps has previously been measured using various techniques, and was reported to have a saturation concentration of the order of $1-7 \times 10^{19} \text{ cm}^{-3}$ [29]–[32]. The out-diffusion of a single Ga atom into the cap will result in the formation of one V_{III} . An identical flux of vacancies will consequently be generated with the same rate at the semiconductor surface due to this flux of Ga out-diffusion. Therefore, to quantify the vacancies in the semiconductor one has to determine the flux of the Ga diffusing into the dielectric cap. The boundary conditions associated with the Ga out-diffusion assume that diffusion governed by (10) and that Ga diffuses into the cap approaching its solubility limit as time goes to infinity [33], with an initial Ga concentration equal to

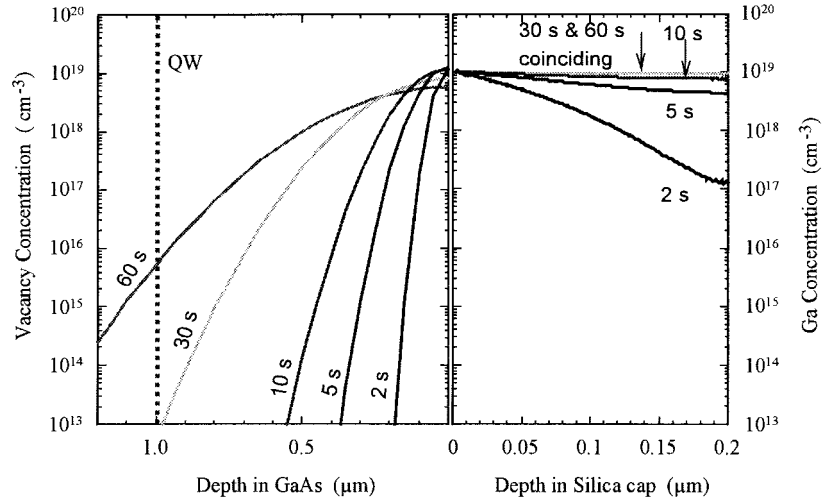


Fig. 5. Plot for the Ga profile in a 200-nm SiO₂ film, and the resulting group-III vacancy profile in the semiconductor for different annealing times at 950 °C.

zero in the cap. The boundary conditions can be expressed as:

$$\begin{aligned} @t=0 &\rightarrow C_{\text{Ga}} = 0 \\ @t \rightarrow \infty &\rightarrow C_{\text{Ga}} = C_{\text{sol}} \\ @z=d &\rightarrow \frac{d}{dx} C_{\text{Ga}} = 0. \end{aligned} \quad (15)$$

The solubility limit of the caps is termed C_{sol} , while d is the thickness of the cap, and is typically of the order of 200 nm. Different, and more complicated, boundary conditions would be necessary to describe the diffusion of Ga in the silica cap while taking into account some of the possibilities such as Ga pile up at the surface of the cap and at the GaAs/cap interface beyond saturation. However, the above boundary conditions can be solved giving a profile expressed as

$$C_{\text{Ga}}(z, t) = \sum_{n=1}^{\infty} k_n \sin[\lambda_n z] \{1 - \exp[-\lambda_n^2 D_{\text{Ga}} t]\} \quad (16)$$

$$k_n = \frac{\langle C_{\text{sol}} \cdot \sin[\lambda z] \rangle}{\langle \sin[\lambda z] \cdot \sin[\lambda z] \rangle} \quad (17)$$

$$\lambda_n = \frac{n\pi}{d} \quad (18)$$

where D_{Ga} is the Ga diffusion coefficient in SiO₂. It was reported to be $5.2 \times 10^{-4} \exp[-1.77/k_B T]$ cm²·s⁻¹, and equal to 2.7×10^{-11} cm²·s⁻¹ at 950 °C. The resulting Ga profiles for various anneal times are plotted in Fig. 5. As can be seen in the figure, the saturation of Ga in the cap takes places after about 10 s of annealing, which matches very well the reported measurements [33]. Due to this Ga flux, there exists a similar flux of vacancy in-diffusion into the semiconductor. Therefore, at the GaAs-SiO₂ interface the following boundary condition should be satisfied

$$D_{\text{vac}} \left. \frac{d}{dz} N_v(z, t) \right|_{z=0} = D_{\text{Ga}} \left. \frac{d}{dz} C_{\text{Ga}}(z, t) \right|_{z=0} \quad (19)$$

where, D_{vac} and $N_v(x, t)$ are the vacancy diffusion coefficient and concentration in the semiconductor, respectively. Using

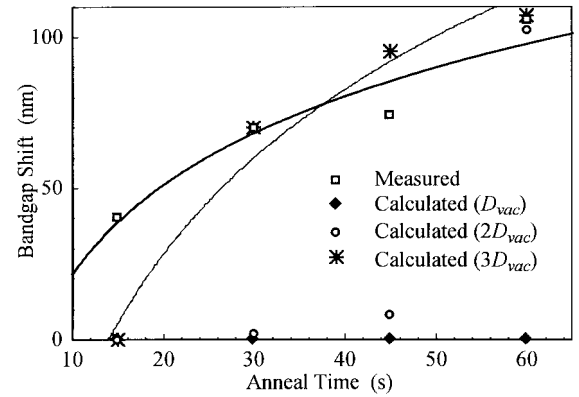


Fig. 6. Plot for measured and calculated PL shifts resulting from the IFVD process in a double QW for different values of D_{vac} .

the Laplace transform to solve the diffusion equation (10), with the boundary conditions in (19) and initial vacancy concentration equal to zero, the vacancy concentration can be expressed as a convolution of two functions [26], such that

$$\begin{aligned} N_v(z, t) &= \int_0^t f(t-\tau) \cdot g(\tau) \cdot d\tau \\ f(t) &= \left. \frac{d}{dx} N_v(z, t) \right|_{x=0} \\ g(t) &= \frac{D_{\text{vac}}}{\sqrt{\pi t}} \exp\left[\frac{-z^2}{4D_{\text{vac}} t}\right]. \end{aligned} \quad (20)$$

The vacancy profile was obtained using the reported D_{vac} , which is 6.1×10^{12} cm²·s⁻¹ at 950 °C. The value of w_v can be then be obtained from (3), and was equal to 15×10^3 hop·s⁻¹ [3]. Also a value of 1×10^{19} cm⁻³ was used as the Ga solubility limit in the silica caps [31]. As can be seen in Fig. 5, the vacancy concentration at the surface decreases as the Ga concentration in the cap saturates, which also explains the commonly observed saturation in the dielectric caps used in IFVD [30], and the effect of the cap thickness on the amount of QWI obtained. Upon evaluating $N_v(d_{\text{QW}}, t)$,

N_{IC} and the associated PL shifts can be calculated in a similar manner to the PIDLI process. For the parameters stated above, the predicted amount of intermixing is negligible for annealing times less than 60 s, as can be seen in Fig. 6. However, if D_{vac} is increased, the predicted intermixing is in better agreement with the measured values. For v equal to $1 \times 10^{-4} \text{ cm} \cdot \text{s}^{-1}$, and a value for D_{vac} three times the reported value, the measured PL shifts are in close agreement with those predicted from the model. Similarly to the argument for the PIDLI process, suggesting a factor of 2–3 change in D_{vac} is within experimental error of the range of values reported.

V. SUMMARY

We have developed an atomic-scale model for the kinetics of intermixing of GaAs–AlGaAs quantum-confined heterostructures starting from first principles. The model hypothesis has been validated by successfully predicting the amounts of QWI induced by the processes of hydrogen plasma induced defect layer intermixing and IFVD, two different techniques for QWI. The results show a good degree of accuracy considering the uncertainty in the parameters used. The predictions are in good agreement with experimental measurements for both processes if the vacancy diffusion coefficient is increased by a factor of 2 to 3 from its reported value. It is obvious that a more rigorous model would take into account effects such as defect recombination, as well as correlation effects in diffusion, and hence predict more accurately the effect of Al–Ga mixing at the interface of the well and barrier. The error function profiles assumed for the diffusion profiles could also be substituted with exact diffusion profiles extracted from the statistical diffusion model. Moreover, the concept of the defect surface recombination velocity should prove useful in characterizing various technological factors such as the state of the surface of the semiconductor.

ACKNOWLEDGMENT

The authors would like to thank B. S. Ooi, E. A. Avrutin, M. W. Street, D. C. Hutchings, and M. Rahman for assistance.

REFERENCES

- [1] W. D. Laidig, N. Holonyak, Jr., M. D. Camras, K. Hess, J. J. Coleman, P. D. Dapkus, and J. Bardeen, "Disorder of an AlAs–GaAs superlattice by impurity diffusion," *Appl. Phys. Lett.*, vol. 38, pp. 776–778, 1981.
- [2] D. G. Deppe and N. Holonyak, Jr., "Atom diffusion and impurity induced layer disordering in quantum well III–V semiconductor heterostructures," *Appl. Phys. Lett.*, vol. 64, pp. R93–R113, 1988.
- [3] K. B. Kahen, D. L. Peterson, G. Rajeswaran, and D. J. Lawrence, "Properties of Ga vacancies in AlGaAs materials," *Appl. Phys. Lett.*, vol. 55, pp. 651–653, 1989.
- [4] S. Y. Chiang and G. L. Pearson, "Properties of vacancy defects in GaAs single crystals," *J. Appl. Phys.*, vol. 46, pp. 2986–2991, 1975.
- [5] I. Gontijo, T. Krauss, J. H. Marsh, and R. M. De La Rue, "Post-growth control of GaAs/AlGaAs quantum-well shapes by impurity-free vacancy diffusion," *IEEE J. Quantum Electron.*, vol. 30, pp. 1189–1195, 1994.
- [6] Y. T. Oh, T. W. Kang, C. Y. Hong, K. T. Kim, and T. W. Kim, "The relation between Ga vacancy concentrations and diffusion lengths in intermixed GaAs/Al_{0.35}Ga_{0.65}As multiple-quantum wells," *Solid State Commun.*, vol. 96, pp. 241–244, 1995.
- [7] W. P. Gillin, A. C. Kimber, D. J. Dunstan, and R. P. Webb, "Diffusion of ion-beam created vacancies and their effect on intermixing—A gambler's ruin approach," *J. Appl. Phys.*, vol. 76, pp. 3367–3371, 1994.
- [8] R. M. Cohen, "Point defects and diffusion in thin films of GaAs," *Mater. Sci. Eng. Rep.*, vol. R20, pp. 167–280, 1997.
- [9] A. C. Bryce, F. Camacho, P. Cusumano, and J. H. Marsh, "CW and mode-locked integrated extended cavity lasers fabricated using impurity free vacancy disordering," *IEEE J. Select. Topics Quantum Electron.*, vol. 3, pp. 885–892, 1997.
- [10] M. W. Street, N. D. Whitbread, D. C. Hutchings, J. M. Arnold, J. H. Marsh, J. S. Aitchison, G. T. Kennedy, and W. Sibbett, "Quantum-well intermixing for the control of second-order nonlinear effects in Al–GaAs multiple-quantum-well waveguides," *Opt. Lett.*, vol. 22, p. 1600, 1997.
- [11] A. Saher Helmy, J. S. Aitchison, and J. H. Marsh, "The kinetics of intermixing of GaAs/AlGaAs quantum confined heterostructures," *Appl. Phys. Lett.*, vol. 71, pp. 2998–3000, 1997.
- [12] J. H. Marsh, P. Cusumano, A. C. Bryce, B. S. Ooi, and S. G. Ayling, "GaAs/AlGaAs photonic integrated circuits fabricated using impurity-free vacancy disordering," *Proc. SPIE*, vol. 74, pp. 2401–2405, 1995.
- [13] P. K. Haff and Z. E. Switkowski, "Ion-beam-induced atomic mixing," *J. Appl. Phys.*, vol. 48, pp. 3383–3386, 1977.
- [14] B. S. Ooi, A. C. Bryce, and J. H. Marsh, "Integration process for photonic integrated-circuits using plasma damage-induced layer intermixing," *Electron. Lett.*, vol. 31, pp. 449–451, 1995.
- [15] C. J. McLean, A. McKee, G. Lullo, A. C. Bryce, R. M. De La Rue, and J. H. Marsh, "Quantum well intermixing with high spatial selectivity using pulsed laser technique," *Electron. Lett.*, vol. 31, pp. 1285–1286, 1995.
- [16] W. Hayes and A. M. Stoneham, *Defects and Defect Processes in Non-Metallic Solids*. New York: Wiley, 1985.
- [17] D. G. Deppe, L. J. Guido, N. Holonyak, Jr., K. C. Hsieh, R. D. Burnham, R. L. Thornton, and T. L. Paoli, "Stripe-geometry quantum well heterostructure Al_xGa_{1-x}As–GaAs lasers defined by defect diffusion," *Appl. Phys. Lett.*, vol. 49, pp. 510–512, 1986.
- [18] B. S. Ooi, K. McIlvaney, M. W. Street, A. Saher Helmy, S. G. Ayling, A. C. Bryce, J. H. Marsh, and J. S. Roberts, "Selective quantum-well intermixing in GaAs/AlGaAs structures using impurity-free vacancy diffusion," *IEEE J. Quantum Electron.*, vol. 33, pp. 1784–1793, 1997.
- [19] R. J. Borg, and G. J. Dienes, *An Introduction to Solid State Diffusion*. New York: Academic, 1988.
- [20] B. S. Ooi, M. W. Street, S. G. Ayling, A. C. Bryce, J. H. Marsh, and J. S. Roberts, "The application of selective intermixing in selective areas SISA technique to the fabrication of photonic devices in GaAs/AlGaAs structures," *Int. J. Optoelectron.*, vol. 10, pp. 257–263, 1995.
- [21] T. E. Schlesinger and T. Kuech, "Determination of the interdiffusion of Al and Ga in undoped (Al, Ga)As/GaAs quantum wells," *Appl. Phys. Lett.*, vol. 49, pp. 519–521, 1986.
- [22] S. Salimian C. Yuen, C. Shih, and C. R. Cooper, "Damage study of dry etched GaAs recessed gates for field effect transistors," *J. Vac. Sci. Technol.*, vol. 9B, pp. 114–119, 1991.
- [23] D. Lootens, P. Vandaele, P. Demeester, and P. Clauws, "The study of electrical damage in GaAs induced by SiCl₄ reactive ion etching," *J. Appl. Phys.*, vol. 70, pp. 221–224, 1991.
- [24] M. Rahman, M. A. Foad, S. Hicks, M. C. Holland, and C. D. W. Wilkinson, "Defect penetration during plasma etching of semiconductors," in *Mater. Res. Soc. Symp. Proc.*, 1993, vol. 279, pp. 775–780.
- [25] M. Rahman, N. P. Johnson, M. A. Foad, A. R. Long, M. C. Holland, and C. D. Wilkinson, "Model for conductance in dry-etch damage n-GaAs structures," *Appl. Phys. Lett.*, vol. 61, pp. 2335–2338, 1992.
- [26] M. D. Greenberg, *Advanced Engineering Mathematics*. Englewood Cliffs, NJ: Prentice-Hall, 1968.
- [27] K. V. Vaidyanathan, M. J. Helix, D. J. Wolfrod, B. G. Streetman, R. J. Blattner, and C. A. Evans Jr., "Study of encapsulants for annealing GaAs," *J. Electrochem. Soc.*, vol. 124, pp. 1781–1784, 1977.
- [28] D. G. Deppe, L. J. Guido, N. Holonyak, Jr., K. C. Hsieh, R. D. Burnham, R. L. Thorton, and T. L. Paoli, "Stripe-geometry quantum well heterostructure Al_xGa_{1-x}As–GaAs lasers defined by defect diffusion," *Appl. Phys. Lett.*, vol. 49, pp. 510–512, 1986.
- [29] S. Wagner and E. I. Povolonis, "Diffusion of Ga through silicon dioxide films into silicon," *J. Electrochem. Soc.*, vol. 121, pp. 1487–1496, 1974.
- [30] X. Wen, J. Y. Chi, E. S. Koteles, B. Elman, and P. Melman, "Processing parameters for selective intermixing of GaAs/AlGaAs quantum wells," *J. Electron. Mater.*, vol. 19, pp. 539–542, 1990.

- [31] T. Haga, N. Tachino, Y. Abe, J. Kasahara, A. Okubora, and H. Hasegawa, "Out-diffusion of Ga and As atoms into dielectric films in SiO_x/GaAs and SiNy/GaAs systems," *J. Appl. Phys.*, vol. 66, pp. 5809–5815, 1989.
- [32] S. Bürkner, M. Maier, E. C. Larkins, W. Rothemund, E. P. O'Rielly, and J. D. Ralston, "Process parameter dependence of impurity-free interdiffusion in GaAs/AlGaAs and InGaAs/GaAs multiple quantum wells," *J. Electron. Mater.*, vol. 24, pp. 805–812, 1995.
- [33] M. Katayama, Y. Tokuda, N. Ando, Y. Inoue, A. Usami, and T. Wada, "X-ray photoelectron spectroscopic study of rapid thermal processing on SiO₂/GaAs," *Appl. Phys. Lett.*, vol. 54, pp. 2559–2562, 1989.

Amr Saher Helmy (S'94) was born in Cairo, Egypt, in 1970. He received the B.Sc. degree in electronics and telecommunication engineering from Cairo University in 1993. In 1994, he was awarded a British Council scholarship to pursue the M.Sc. degree in electronics and electrical engineering at the University of Glasgow, Glasgow, Scotland, U.K. He is currently working toward the Ph.D. degree in the same department.

His contribution in the NATO school "New Trends in Terahertz Technology" won the best student poster prize. His main research interests include linear and nonlinear guided wave integrated optoelectronics using quantum-well intermixing.

He was awarded the Francis Morrison prize for outstanding performance.

J. Stewart Aitchison (M'96) received the B.Sc. and Ph.D. degrees from The Physics Department, Heriot-Watt University, Edinburgh, Scotland, U.K., in 1984 and 1987, respectively. His dissertation work was on optical bistability in semiconductor waveguides.

From 1988 to 1990, he was a post-doctoral Member of Technical Staff with Bellcore, NJ. His research interests were in the areas of highly nonlinear glasses and spatial soliton propagation. He joined The Department of Electronics and Electrical Engineering at The University of Glasgow, Glasgow, Scotland, U.K., in 1990 as a Lecturer and was promoted to Senior Lecturer in 1995. Since his appointment at The University of Glasgow, he has developed his interests in nonlinear optical waveguides. In particular, III–V semiconductors operated at the half bandgap for optical switching and soliton propagation. More recently, his attention has focused on second-order effects for all-optical switching and frequency conversion applications. He has also developed research interests in planar silica technology for photosensitivity, waveguide lasers and passive components. In 1996, he was the holder of a Royal Society of Edinburgh Personal Fellowship to carry out research on spatial solitons. He is the author or co-author of over 200 refereed journal and conference papers.

Dr. Aitchison is a member of the Institute of Physics the Optical Society of America and IEEE Lasers and Electro-Optics Society.

John H. Marsh (M'91–SM'91), for photograph and biography, see this issue, p. 583.